Icarus 326 (2019) 151–161

Contents lists available at ScienceDirect

Icarus

journal homepage: www.elsevier.com/locate/icarus

Evidence for recent and ancient faulting at Mare Frigoris and implications for lunar tectonic evolution

Nathan R. Williams[a,b,*], James F. Bell III[a], Thomas R. Watters[c], Maria E. Banks[c,d], Katie Daud[c], Renee A. French[e,f]

[a] School of Earth and Space Exploration, Arizona State University, Tempe, AZ, USA
[b] Jet Propulsion Laboratory, California Institute of Technology, Pasadena, CA, USA
[c] Center for Earth and Planetary Studies, Smithsonian Institution, Washington, DC, USA
[d] NASA Goddard Space Flight Center, Greenbelt, MD, USA.
[e] Northwestern University, Department of Earth and Planetary Sciences, Evanston, IL, USA
[f] Oakton Community College and Harold Washington College, Chicago, IL, USA

ARTICLE INFO

Keywords:
Tectonics
Moon
Geophysics
Scarp
Ridge
Graben
Mare
Frigoris

ABSTRACT

Nearside basin-related extensional tectonism on the Moon was thought to have ended by about 3.6 billion years ago and mare basin-localized contractional deformation ended by about 1.2 billion years ago. Lunar Reconnaissance Orbiter Camera (LROC) high resolution (50–200 cm/pixel) images show the Moon's surface in unprecedented detail and have enabled us to find many previously unidentified tectonic landforms, forcing a re-assessment of our views of tectonism in the maria. The morphology and stratigraphic relationships of these newly identified populations of tectonic landforms imply a more complex and longer-lasting history of deformation. We selected Mare Frigoris as an ideal location to perform a mapping survey where excellent imaging conditions, abundant tectonic landforms, and restricted mascon allow us to unravel the mare's tectonic evolution. Similar to previous surveys, we find that tectonism in the eastern portion of Mare Frigoris was controlled by ancient mascon induced flexure. In the western portion, however, we identify a parallel set of ancient compressional wrinkle ridges across the mare that is inconsistent with an origin by mare basin-centric mascon flexure or influence from the Mare Imbrium mascon. Instead, our results imply an ancient, regional, non-isotropic stress field over western Mare Frigoris. We also identify young wrinkle ridges and show that they have likely been active within the last 1 billion years, and some ridges as recently as within 40 million years. Finally, we identify a 300 km long series of lobate scarps coincident with one of the shallow moonquakes recorded during Apollo and use geodetic strain from the mapped global population of young lobate scarps to predict a level of seismicity consistent with the shallow moonquakes recorded during Apollo. In tandem with similarly young lobate scarps and small graben, as well as recorded shallow moonquakes, these young wrinkle ridges imply that some tectonism in and around Mare Frigoris has occurred in the geologically recent past and likely still continues today.

1. Introduction

Tectonism in the lunar maria is largely thought to be controlled by flexure and induced subsidence to compensate large mascons – or mass concentrations (Melosh, 1978; Solomon and Head, 1979, 1980). Previous studies also concluded that tectonism in the lunar maria occurred long ago, with extension ceasing by ~3.6 billion years ago and compression by ~1.2 billion years ago (Lucchitta and Watkins, 1978; Solomon and Head, 1979, 1980; Hiesinger et al., 2003). However, some mare-filled topographic basins that are not necessarily impact structures – most notably Oceanus Procellarum and western Mare Frigoris – that lack large super-isostatic (unequilibrated) mascons are observed to have compressional tectonic landforms that do not conform to the classical mascon-related patterns. Additionally, some mare tectonic landforms have remarkably crisp morphologies not previously observed, suggestive of more recent activity. Understanding the occurrence of these features via their distribution and morphology is therefore essential to reconstructing the thermal-tectonic-magmatic evolution of the Moon.

The enigmatic Mare Frigoris (Fig. 1), located north of Mare Imbrium

* Corresponding author at: Jet Propulsion Laboratory, California Institute of Technology, Pasadena, CA, USA.
E-mail address: Nathan.R.Williams@jpl.nasa.gov (N.R. Williams).

https://doi.org/10.1016/j.icarus.2019.03.002
Received 25 January 2016; Received in revised form 30 August 2018; Accepted 4 March 2019
Available online 07 March 2019
0019-1035/ © 2019 Elsevier Inc. All rights reserved.

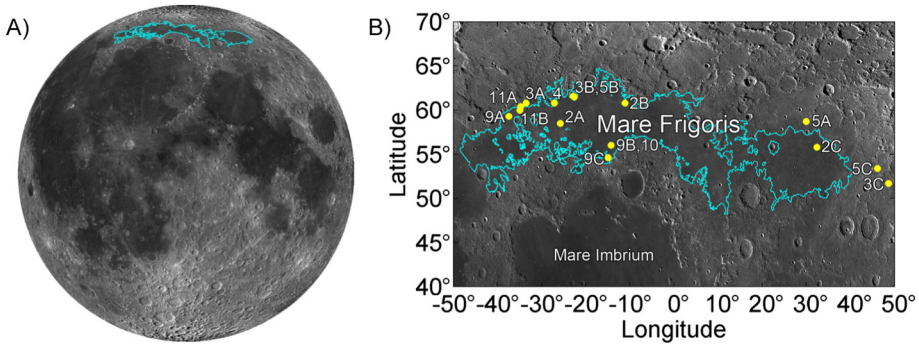


Fig. 1. A) LROC Wide Angle Camera (Robinson et al., 2010) global mosaic orthographic projection centered at the sub-Earth point (0°N, 0°E) showing the location of Mare Frigoris (mare boundary outlined in teal) on the northern nearside (Nelson et al., 2014). B) LROC Wide Angle Camera global mosaic equirectangular projection map showing locations of tectonic landform examples in the following figures. (For interpretation of the references to color in this figure legend, the reader is referred to the web version of this article.)

is an irregularly-shaped large mare-filled topographic basin. The western two-thirds of the mare lack a large super-isostatic load, while the eastern third of the mare has a large central super-isostatic load. Yet, the entire mare exhibits abundant examples of each type of lunar tectonic landform (i.e., wrinkle ridges, lobate scarps, and graben; see details in the following section). Some of the landforms also interact with each other both spatially and temporally, providing greater insight to their respective and sometimes linked origins. Mare Frigoris's diverse suite of landforms and spatially variable mascon flexure influence make it an ideal location to study the occurrence of these features. In this study, we map the tectonic landforms in Mare Frigoris and the adjacent highlands to reconstruct the tectonic history of Mare Frigoris as a type area – unraveling the distribution, controls, and timing of tectonic activity to serve as a baseline for understanding many other tectonic landforms elsewhere on the Moon in both the mare and highlands without clear impact structural control.

2. Background

Tectonic landforms on the Moon are expressed through three principal morphologic classifications: wrinkle ridges, lobate scarps, and graben. Wrinkle ridges are curvilinear to sinuous raised relief landforms comprised of a broad arch with a superimposed narrow crest (Fig. 2) (e.g., Gilbert, 1893; Lucchitta, 1976a, 1976b; Plescia and Golombek, 1986; Watters and Johnson, 2010). Wrinkle ridge heights reach up to several hundred meters and lengths reach up to over a hundred kilometers (Watters, 1988; Golombek et al., 1991; Watters and Johnson, 2010). They occur exclusively in mare deposits and have been interpreted to be surface expressions of complex thrust faulting and folding, although the subsurface structure is debated (Golombek et al., 1991; Watters, 1992; Schultz, 2000; Golombek et al., 2001; Mueller and Golombek, 2004; Watters, 2004). In large impact basins like Imbrium, wrinkle ridges typically occur radial or concentric to the center of the basin and have been proposed to form as a result of subsidence and flexure from isostatic compensation soon after emplacement of mare basalts (e.g., Melosh, 1978; Solomon and Head, 1979, 1980; Byrne et al., 2015).

Lunar lobate scarps are curvilinear to arcuate raised relief landforms, but in contrast to wrinkle ridges, lobate scarps have simple asymmetric morphologies consisting of one steep face and a gently sloping back limb (Fig. 3) (e.g., Binder and Gunga, 1985; Banks et al., 2012). They are also interpreted to be surface expressions of thrust faults, but simpler and with much less folding than wrinkle ridges (Binder and Gunga, 1985; Watters et al., 2010; Williams et al., 2013). Lunar lobate scarps have typical heights of tens of meters with some over a hundred meters in relief. Typical lengths of individual lobate scarps are only a few to tens of kilometers, although grouped series of scarps collectively can have much greater extents, some spanning several hundreds of kilometers (Binder and Gunga, 1985; Banks et al., 2012). They occur throughout the highlands at all latitudes and are observed in the maria, except at mare-highland boundaries where lobate scarps sometimes transition to more complex wrinkle ridge morphologies (Fig. 4) (Howard and Muehlberger, 1973; Lucchitta, 1976a, 1976b; Watters, 1988; Watters et al., 2010). For example, the Lee-Lincoln scarp in the valley of Taurus-Littrow near the Apollo 17 landing site is a well-documented lobate scarp that transitions into a more complex wrinkle ridge-like morphology on the mare-filled valley floor (Schmitt and Cernan, 1973; Scott, 1973; Lucchitta, 1976a, 1976b; Watters and Johnson, 2010).

Lunar graben (also called “linear rilles” in some literature) are linear to arcuate negative relief landforms consisting of two steep sides creating a trough, typically with a flat floor (Fig. 5) (McGill, 1971; Golombek, 1979). Large graben have typical depths of several hundred meters, widths of hundreds of meters to over a kilometer, and lengths of

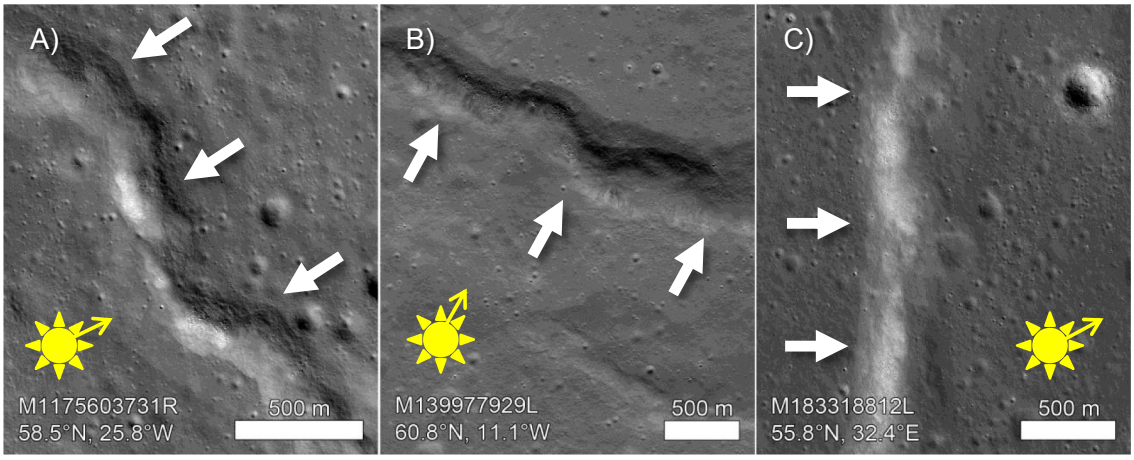


Fig. 2. Examples of degraded lunar wrinkle ridge crests (white arrows) in Mare Frigoris.

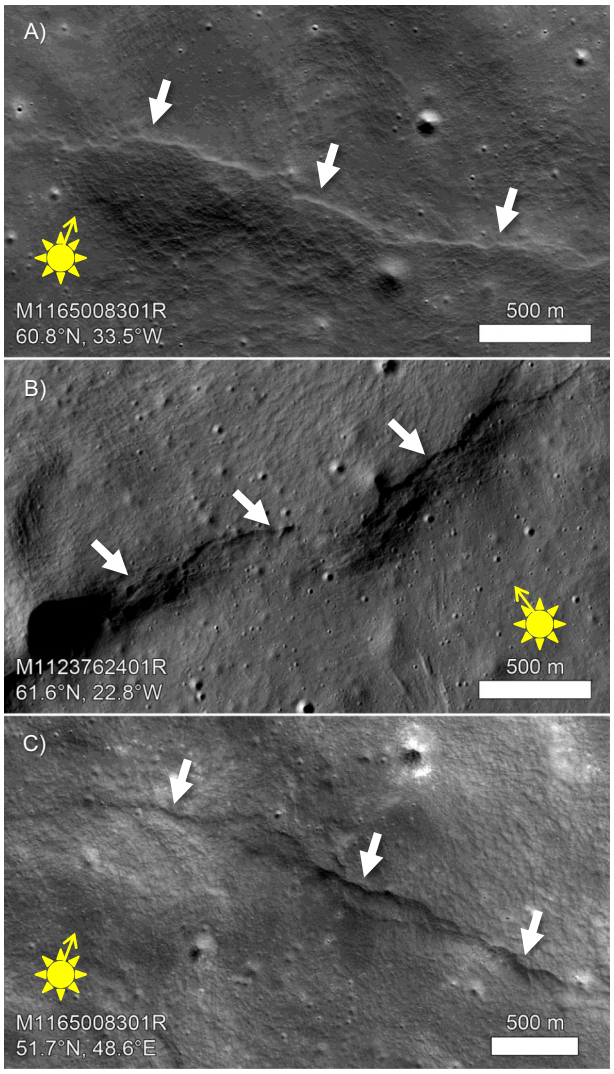


Fig. 3. Examples of lunar lobate scarps (white arrows) in the highlands adjacent to Mare Frigoris.

up to several hundred kilometers (Watters and Johnson, 2010). These large graben occur in both the maria and the neighboring highlands, and typically have basin-concentric or basin-radial orientations (McGill, 1971; Golombek, 1979; Wilhelms, 1987). Large graben are therefore inferred to form as a result of flexure from isostatic compensation as the extensional counterpart to compressional wrinkle ridges (Melosh, 1978; Solomon and Head, 1979, 1980). Recently, a globally distributed population of very small graben has been discovered using LROC NAC images (Watters et al., 2012). Small graben globally have typical depths and widths of only a few to a few tens of meters (average 26 m) and lengths of hundreds of meters (average 179 m) (Watters et al., 2012; French et al., 2015). Based on infilling rates of 2–8 cm/million years for shallow depressions in lunar regolith (Arvidson et al., 1975), a ~1 m deep graben should be filled within ~12.5–50 million years. These small-scale graben commonly occur in clusters and are often associated with wrinkle ridges and lobate scarps (Watters et al., 2012; French et al., 2015).

Mare Frigoris is an excellent site to study the aforementioned landforms, as all occur in or around the mare and in areas with variable influence from mascon flexure. Mare Frigoris is filled with mare basalts ranging in age from ~2.6 to 3.8 billion years old, with most being ~3.4–3.8 billion years old (Hiesinger et al., 2010). Basalts in the eastern part of the mare tend to be older (mostly ~3.6–3.8 billion years

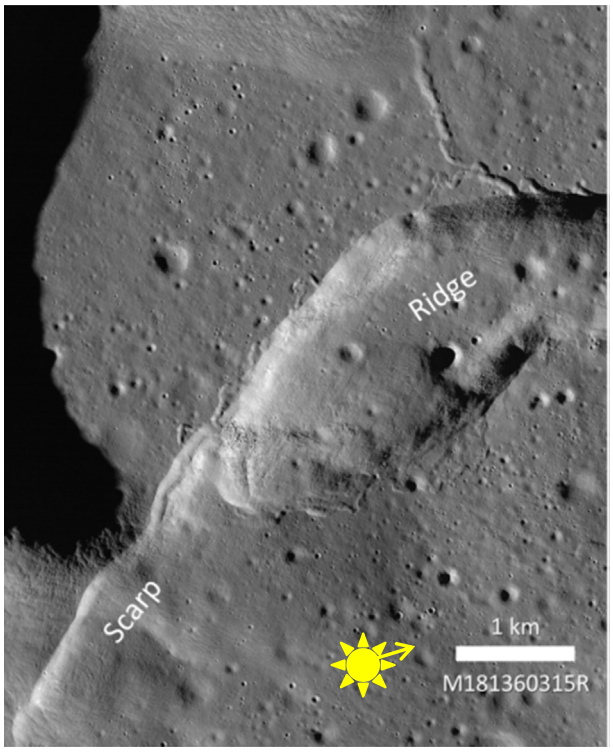


Fig. 4. LROC NAC image showing a wrinkle ridge transitioning to a lobate scarp along the mare-highland boundary in northwestern Mare Frigoris (60.8°N, 27.1°W).

old) while basalts in the western part of the mare tend to be somewhat younger (mostly ~3.4–3.6 billion years old). Many basins hosting mare are circular or slightly elliptical in shape and formed during large impacts (Wilhelms, 1987). In contrast, the highly elongate and irregular shape of Mare Frigoris does not support an origin as a single impact basin structure even though it is a topographic depression (Whitford-Stark, 1990).

Cadogan (1974, 1975) and Whitaker (1981) proposed that the Mare Frigoris topographic depression is the remnant edge of an ancient (pre-Nectarian) gargantuan impact basin bounded by northern Mare Frigoris, western Oceanus Procellarum, southern Mare Cognitum, and southeastern Mare Vaporum. Such an old, large impact basin would be consistent with the prevalence of mare volcanism on the lunar nearside, thinner nearside crust, distribution of KREEP materials, and low Al/Si ratio in Imbrium ejecta.

The putative Procellarum basin boundary is discontinuous, lacks indicative impact signatures such as an obvious circular to elliptical shape, peak ring structures (for a complex crater), or ejecta blanket, and it is not a mascon. Using GRAIL gravity gradiometry, Andrews-Hanna et al. (2014) identified a polygonal zone of density contrasts along the previously proposed boundaries of the Procellarum basin. A polygonal boundary is not expected for large impacts which should be circular or elliptical. To explain the polygonal structure, Andrews-Hanna et al. (2014) proposed that the Procellarum basin, including Mare Frigoris, may instead be part of a rift system flooded with dense mare basalts. Such a rift system should produce primarily extensional structures subparallel to the main spreading center during rifting, but remnant mare deposits might not be fully isostatically compensated by the crust even long after erupting.

In contrast to Procellarum-related hypotheses, Whitford-Stark (1981, 1990) proposed that the topographic depression of western Mare Frigoris might instead have formed by collapse of a large highlands block into the Imbrium impact cavity. In a block rotation model, the newly formed Frigoris topographic basin would have its lowest

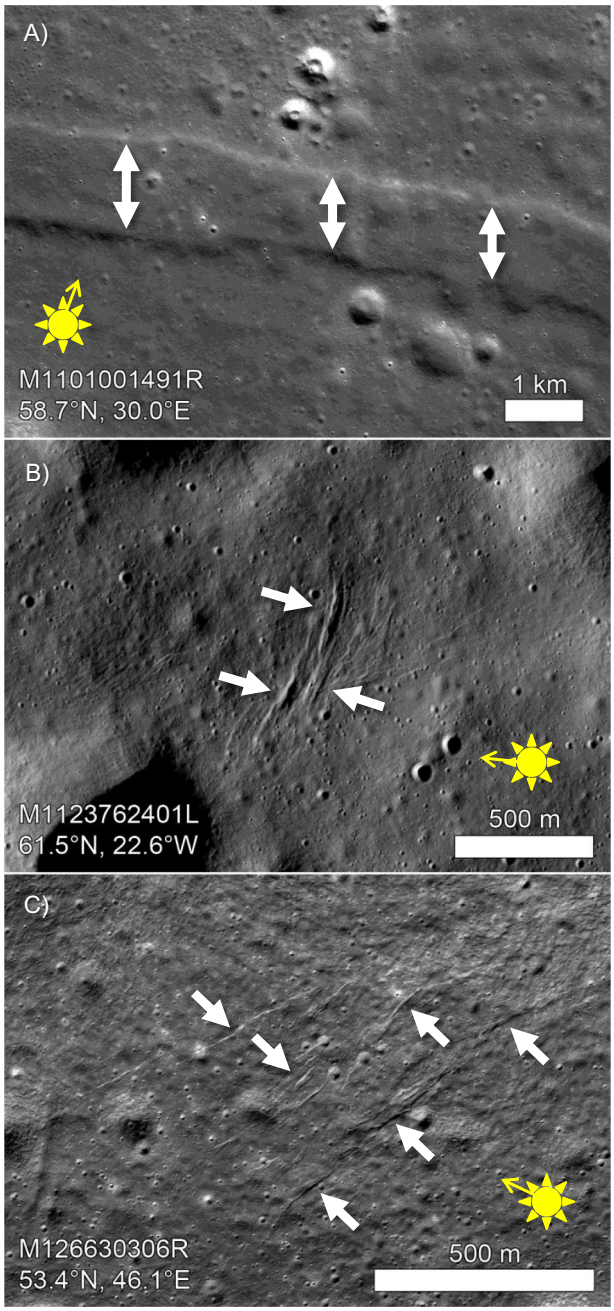


Fig. 5. Examples of a large graben (A, white arrows span width) and two clusters of small graben (B and C, white arrows) in Mare Frigoris.

topography at the distal end of the slump – away from Imbrium and towards Frigoris's northern rim. That deeper part of the proto-Frigoris basin could then accommodate a thicker basaltic fill. After filling with mare, that dense basaltic fill would place a load on the crust to preferentially cause subsidence, flexure, and faulting over the thickest fill in the north. A preferential development of wrinkle ridges in thicker mare deposits along the northern boundary of western Mare Frigoris would be consistent with block rotation in support of a collapse model. Whitford-Stark also noted that tectonic structures in the eastern part of Mare Frigoris have a pattern consistent with an impact basin, highly degraded and infilled with mare basalts continuous in extent with the mare fill in the non-impact western part of the mare.

Previous studies of Mare Frigoris, however, were limited by the availability of high resolution images at optimal lighting conditions. Whitford-Stark (1990) previously performed a tectonic survey of the mare with limited Lunar Orbiter and Earth-based photographs. High resolution Apollo images were not available due to those missions' equatorial orbits. The Lunar Orbiter photographs for Mare Frigoris, particularly of the eastern mare, were of poor quality in both resolution and lighting that limited morphologic discrimination. Study of high latitude areas of Mare Frigoris were also limited by the highly oblique angles of Earth-based imaging. As a result, many tectonic landforms, especially small-scale examples, could not be identified and their numbers, stratigraphic relationships, and spatial distribution within Mare Frigoris were poorly understood. Two decades later, new imaging has enabled us to resurvey and better understand the distribution and character of tectonic landforms in Mare Frigoris.

3. Data and methods

In 2009, NASA's Lunar Reconnaissance Orbiter was launched into orbit of the Moon. Onboard, the Lunar Reconnaissance Orbiter Camera (LROC) Narrow Angle Cameras (NACs) acquire high resolution (50–200 cm/pixel from 50 to 200 km altitude, resp.) panchromatic images of the lunar surface (Robinson et al., 2010). Due to the spacecraft's polar orbit, LROC can acquire images at all latitudes and variable lighting conditions. The polar orbit also allows for more frequent flyovers and image acquisitions at higher latitudes. At ~60°N, Mare Frigoris occurs far enough north that it has nearly complete image density, but is not too high latitude to suffer from extreme solar incidence and shadows that limit morphological studies.

We selected over 12,000 LROC NAC images across Mare Frigoris to gain nearly complete (~99%) coverage over the mare and the adjacent highlands. Our image selection was restricted by solar incidence angle (55°–85°) and excluded any images acquired during large off-nadir slews by the spacecraft. The selected images were then calibrated, map projected, and resampled to 3 m/pixel using the United States Geological Survey's Integrated System for Imagers and Spectrometers (Anderson et al., 2004). We imported and mosaicked images in a graphical information system and performed a survey of the selected LROC NAC images (for image coverage, see masked area in Fig. 6). Features associated with Mare Imbrium, specifically wrinkle ridges interior to Mare Imbrium and Valles Alpes, were excluded from our survey.

Tectonic landforms were classified as either wrinkle ridges, lobate scarps, large graben, and small graben and vectorized as polylines comprised of multiple line segments. Polylines for wrinkle ridge segments were drawn along the center of the ridge crest. Polylines for lobate scarps were drawn at the base of the scarp face. Polylines for both large and small graben were drawn along the middle of the trough floor. Polylines for all the different tectonic landforms types were drawn with variable lengths to best capture continuous segments of each landform with a nearly constant azimuth.

In our results maps below, we used a 100 m/pixel LROC Wide Angle Camera (WAC) global mosaic (Robinson et al., 2010) and stereo digital elevation model (Scholten et al., 2012) (Fig. 6), and a degree and order 900c Gravity Recovery and Interior Laboratory (GRAIL) free air anomaly map (Lemoine et al., 2014) (Fig. 8).

4. Results

Tectonic patterns differ greatly between the eastern and western parts of Mare Frigoris (Figs. 6–8) with a change in tectonic regime around the 15°E meridian. East of ~15°E, wrinkle ridges (red lines in Fig. 6) occur in a polygonal pattern at the center of the mare. Large linear to arcuate graben (yellow lines in Fig. 6) occur to the north and east of the wrinkle ridges, with most oriented concentric to the center of the wrinkle ridge cluster. These eastern mare tectonic landforms tend to be degraded with broadly undulating topography, shallow slopes, numerous superimposed impact craters, and few small craters (< 100 m diameter) that appear crosscut. A few wrinkle ridges in eastern Mare Frigoris also appear to have superposed small troughs interpreted as

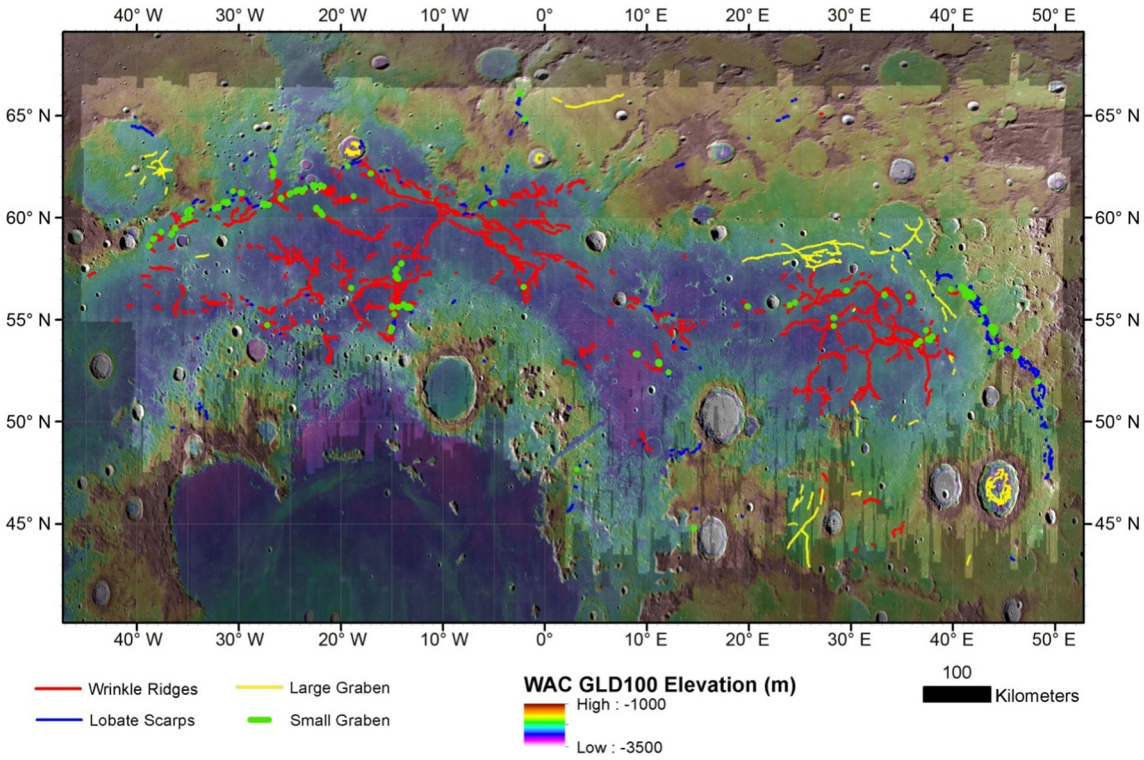


Fig. 6. Tectonic map of Mare Frigoris over LROC WAC GLD100 colorized shaded relief. Shaded mask indicates the boundary of LROC NAC image coverage used in this survey. Small graben are plotted atop lobate scarps and wrinkle ridges such that the ridges and scarps may appear discontinuous but are actually continuous with superimposed graben. (For interpretation of the references to color in this figure legend, the reader is referred to the web version of this article.)

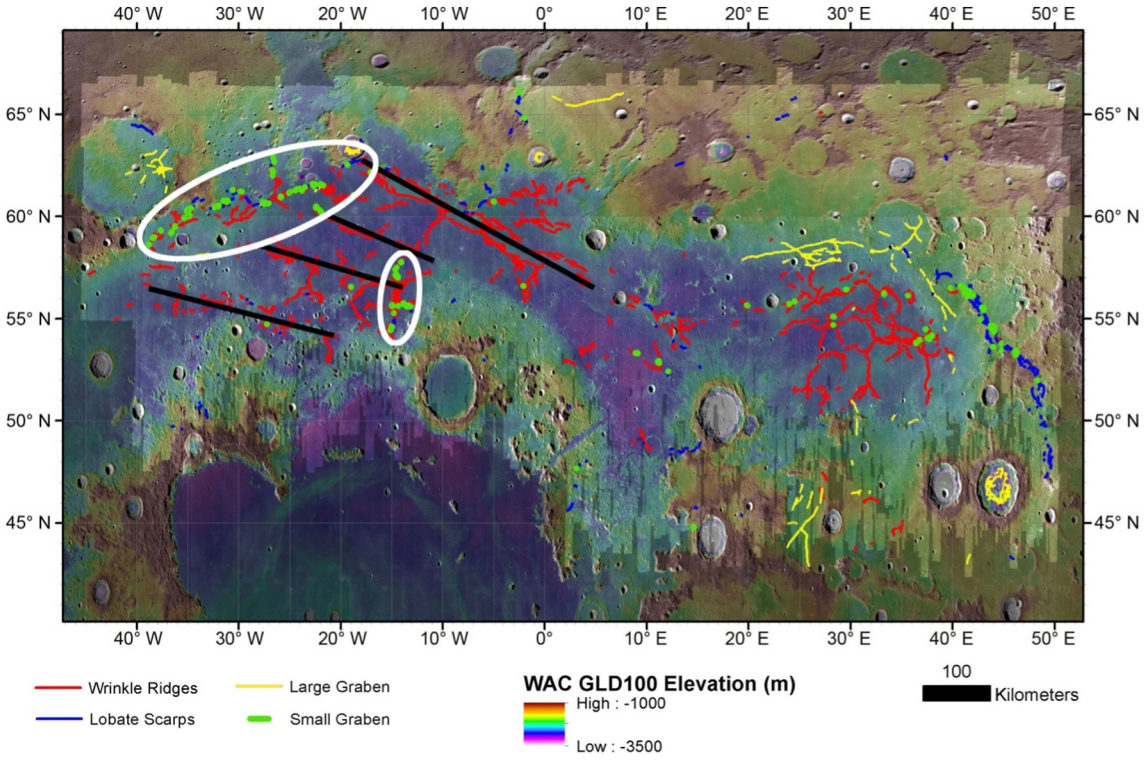


Fig. 7. Tectonic map (same as seen in Fig. 6) with black line overlays indicating parallel sets of degraded wrinkle ridges in western Mare Frigoris, and white circle overlays indicating crisp, young wrinkle ridges.

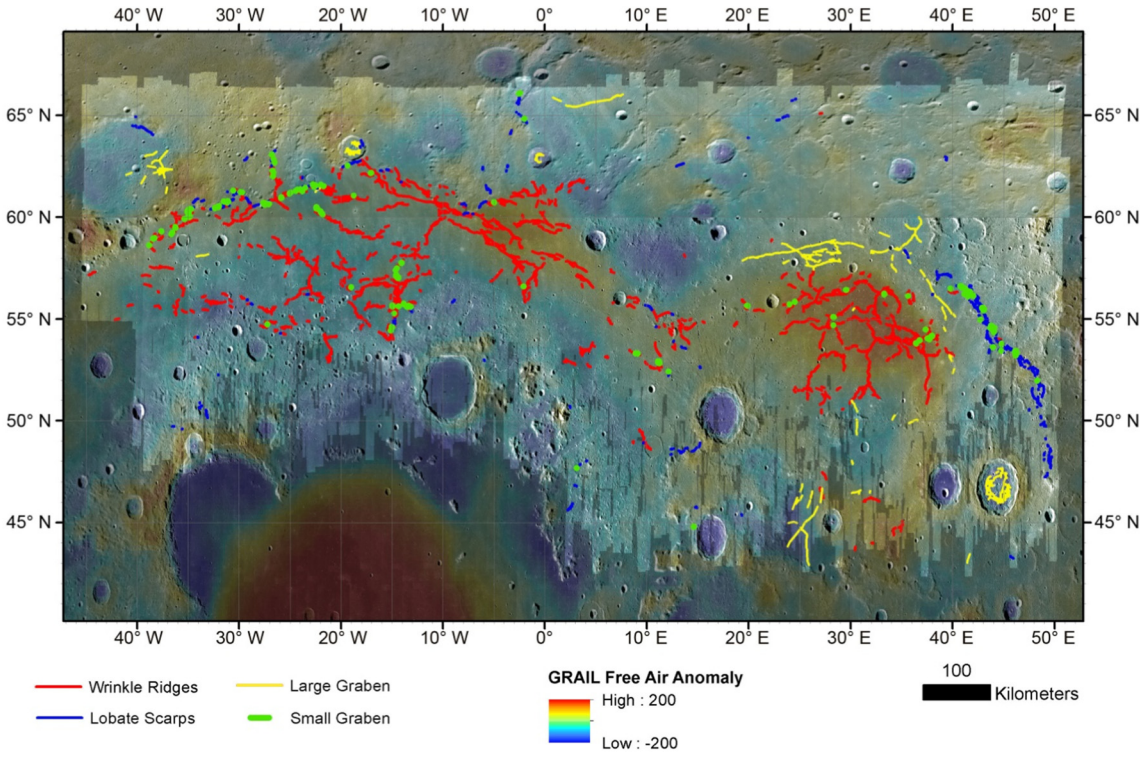


Fig. 8. Tectonic map overlain on GRAIL free-air anomaly map with shaded relief (Zuber et al., 2013; Lemoine et al., 2014). Free-air anomalies are due to excess mass, typically from topography and/or variable crustal density.

small-scale graben (indicated by short green lines in Fig. 6), and also appear to be degraded as their morphology is not as crisp as that of other small graben identified in western Mare Frigoris or globally.

In contrast to the eastern mare, we find that west of ~15°E, Mare Frigoris has two assemblages of tectonic landforms. The first is a set of subparallel wrinkle ridges trending northwest-southeast across the mare (black lines in Fig. 7). Similar to the wrinkle ridges in eastern Mare Frigoris, they appear more degraded with broadly undulating topography, shallow slopes, numerous superimposed impact craters, and no small (< 100 m diameter) crosscut craters. The northeastern-most strands of wrinkle ridges in this set have the greatest relief and are the most continuous, whereas the southwesternmost strands are discontinuous and appear to have lower relief.

We also find that western Mare Frigoris has a distinct population of wrinkle ridges with crisp morphologies (white circles in Fig. 7, examples in Fig. 9) that were not well resolved and/or well illuminated in previous studies. These wrinkle ridges have relatively steep slopes with abrupt changes in slope (for example, Fig. 10 shows a wrinkle ridge with a 17° slope with a sharp break at the base of its crest), few large (> 400 m diameter) superimposed impact craters, and crosscut ~70 small (< 100 m diameter) craters. The morphologically crisp wrinkle ridges tend to occur near the mare-highland boundary, but can extend over 60 km into the mare.

The preferred orientation of wrinkle ridges in western Mare Frigoris by length-weighted circular mean is 285°/105° measured clockwise from north and is statistically significant with p value of < 0.05 calculated using a circular Student's t-test (Fig. 11) (Berens, 2009). Each of the different parallel sets of wrinkle ridges indicated in Fig. 7 have similar mean orientations of 107°, 101°, 96°, and 116° in order from the southwest to northeast. At the mare-highland boundary, these wrinkle ridges sometimes transition to simpler lobate scarp morphologies that continue into the highlands (Fig. 4).

Lobate scarps are also observed in the highlands around Mare Frigoris, both transitioning from mare wrinkle ridges and as

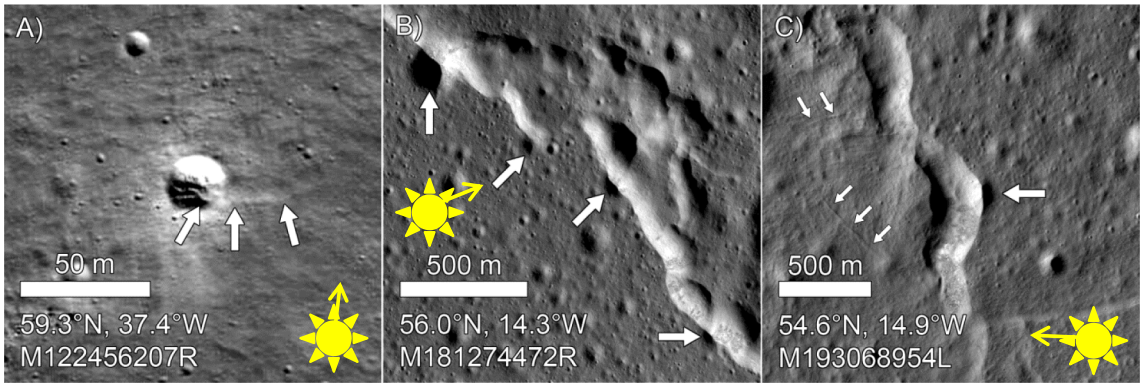


Fig. 9. LROC NAC images showing wrinkle ridges crosscutting small craters. A) A very small wrinkle ridge (arrows) crosscuts a 21 meter diameter crater with bright ejecta. B) A larger wrinkle ridge crosscuts craters (arrows) with diameters of 190 m, 90 m, 100 m, and 80 m from left to right. C) A ~150 m diameter crater (larger white arrow) with an indistinct rim almost completely thrust over by a wrinkle ridge with small shallow graben along the ridge flank (smaller white arrows).

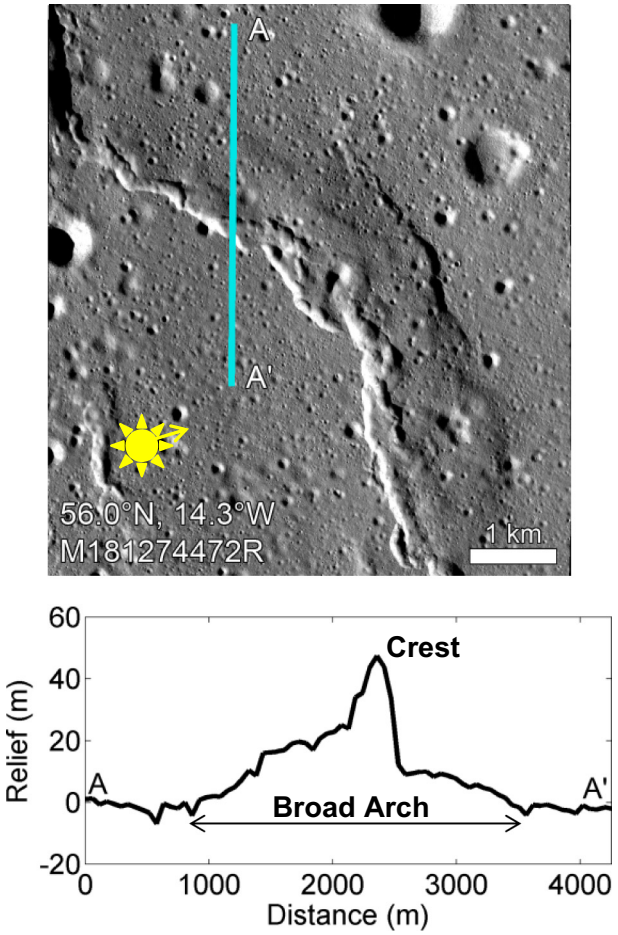


Fig. 10. LROC NAC image showing mare wrinkle ridges with crisp morphologies. A topographic profile from the Lunar Orbiter Laser Altimeter (Smith et al., 2010), indicated as A-A' in teal, shows wrinkle ridge relief consisting of a sharp crest superimposed atop a broad arch (after subtraction of the regional slope). Vertical exaggeration of the plot is 25×. True slope on the ridge face is ~17°. (For interpretation of the references to color in this figure legend, the reader is referred to the web version of this article.)

independent landforms (blue lines in Fig. 6), that were not identified in previous studies. These lobate scarps, like other lobate scarps globally, are very crisp in morphology having steep slopes with sharp changes in slope, few superimposed large (> 400 m diameter) craters, and numerous small (< 100 m diameter) crosscut craters. The largest series of lobate scarps occurs just east of Mare Frigoris from 57°N, 40°E to 47°N, 50°E. It is over 300 km long and generally split along two paired subparallel strands of scarp segments with opposite asymmetries with scarp faces oriented predominantly outwards from the scarp series' central axis.

Over 500 small graben in Mare Frigoris are exclusively associated with lobate scarps and wrinkle ridges (with distances < 5 km), particularly the crisp wrinkle ridges in western Mare Frigoris (white circles in Fig. 7). Small graben in Mare Frigoris typically have widths of only a few meters across and lengths of tens to a few hundred meters. Their depths are not clearly resolved in available stereo topography from LROC (Robinson et al., 2010) or altimetry from LOLA (Smith et al., 2010). Assuming initial surface slopes of at most the angle of repose (perhaps ~30°), we conclude that these small graben have smaller depths than widths and must be less than a few meters deep. The graben have preferred orientations perpendicular and perhaps to a lesser degree parallel to the nearest ridge or scarp, with relatively fewer having oblique geometries (Figs. 12 and 13).

5. Discussion

Eastern Mare Frigoris, with its central polygonal pattern of ridges and more distal large concentric graben, is consistent with classic mascon tectonics (see Melosh, 1978; Solomon and Head, 1979, 1980; Whitford-Stark, 1990; Freed et al., 2001). There is no clear circular topographic ring indicative of an impact, but a moderate (albeit non-circular) positive gravity anomaly does occur (Fig. 8) (Zuber et al., 2013; Neumann et al., 2015). This may have been enabled by mantle uplift under a now heavily degraded ancient impact basin, by thick infilling of mare basalt, or by significant intrusion of high-density magmas. The heavily degraded appearance of both the wrinkle ridges and large graben in this area is consistent with flexure having occurred long ago, bounded by but perhaps soon after mare emplacement. In particular, the occurrence of degraded large graben in Mare Frigoris is notable. Based on global crosscutting relations, large-scale graben formation stopped globally ~3.6 billion years ago due to a change from net global expansion to contraction (Solomon and Head, 1979, 1980; Kirk and Stevenson, 1989; Pritchard and Stevenson, 2000). We therefore infer that a significant proportion of isostatic flexure in eastern Mare Frigoris occurred prior to 3.6 billion years ago. The lack of large graben and relatively sparser wrinkle ridges along the southeastern edge of Mare Frigoris suggests that flexure may have been limited there, perhaps due to greater structural rigidity or lithospheric thickness closer to Mare Imbrium and/or Mare Serenitatis (Wieczorek et al., 2013). Alternatively, the younger (< 3.6 billion year old (Hiesinger et al., 2010)) lavas in southeastern Mare Frigoris may have buried any pre-existing structures, particularly infilling topographically lower large graben that are thought to have formed before 3.6 billion years ago.

In contrast, we find that wrinkle ridges in western Mare Frigoris do not support an origin by mascon induced flexure. Horizontal principal stress components for mascon induced flexure should be oriented concentric and/or radial to the mare interior (Melosh, 1978; Solomon and Head, 1979, 1980; Freed et al., 2001). Instead, parallel wrinkle ridges across western Mare Frigoris (black lines in Fig. 7) have a significant preferred orientation of 285°/105° (Fig. 11) which indicates that the greatest compressional horizontal principal stress component across the mare was oriented perpendicular to the ridges (ENE-WSW) at the time of fault formation. The typical degraded appearance of these parallel wrinkle ridges is similar to that of the degraded wrinkle ridges in eastern Mare Frigoris, as well as many other wrinkle ridges elsewhere on the Moon, suggesting that they are a similar ancient age and most likely formed soon after emplacement of the mare basalts.

The northeasternmost of the parallel wrinkle ridges is approximately tangential to Mare Imbrium. This was previously cited to argue for a gradually thicker mare fill towards the northern side of Mare Frigoris and proposed to represent a collapsed and rotated highlands block into Imbrium's impact cavity to the south (Whitford-Stark, 1990). In a block rotation collapse model, the lowest topography would occur at the distal end of the slump – away from Imbrium and towards Frigoris's northern rim. That deeper part of the proto-Frigoris topographic basin could then accommodate a thicker basaltic fill. After filling with mare, that dense basaltic fill would place an uncompensated load on the crust to preferentially cause subsidence, flexure, and faulting over the thickest fill in the north. The widespread occurrence of faults expressed as wrinkle ridges now shown throughout Mare Frigoris suggests that the fill may not be excessively thicker at the northern end, and thus suggests against an Imbrium-triggered crustal collapse and rotation model. The parallel wrinkle ridges farther west across Mare Frigoris also have oblique orientations with respect to the rim of Mare Imbrium, neither concentric nor radial and also inconsistent with flexure induced by Imbrium's mascon.

Wrinkle ridges in the parallel set have decreasing relief and continuity away from the northeasternmost ridge, which suggests that they formed in the same regional, non-isotropic stress regime but with

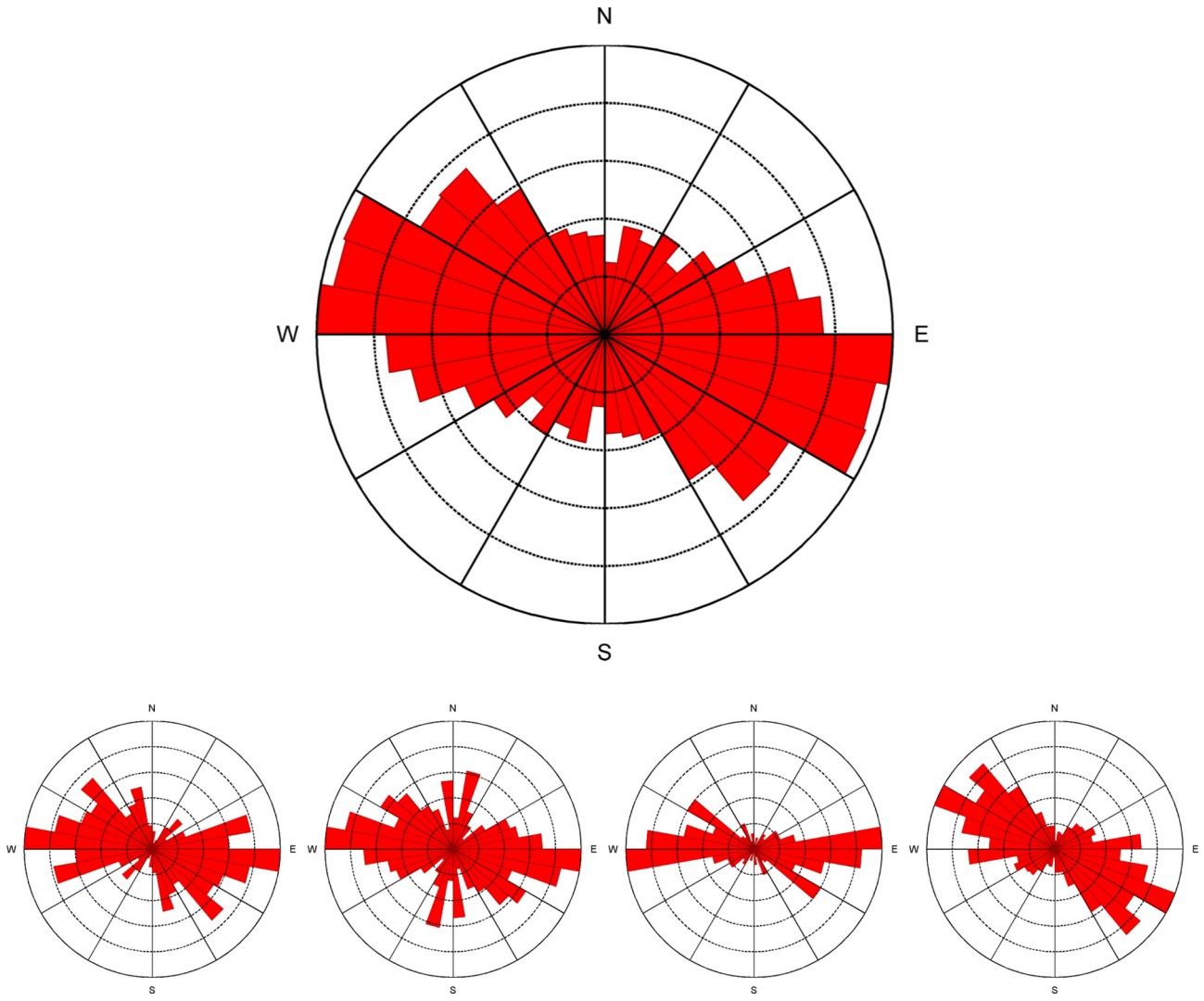


Fig. 11. Rose diagrams showing length-weighted distribution of (top) all wrinkle ridge orientations in Mare Frigoris west of the 15°E meridian and (bottom row) within each set of wrinkle ridges indicated by black lines in Fig. 7 in order from bottom-left being the southwest set and the bottom-right being the northeast set.

decreasing contractional strain with distance towards the south and west. Such a large-scale stress field could be accomplished, for example, by a gargantuan impact structure (Whitaker, 1981) or by rifting (Andrews-Hanna et al., 2014). However, we do not find evidence directly suggesting a giant impact control, such as the "Procellarum basin" (Whitaker, 1981). Some positive gravity anomalies in Oceanus Procellarum are proposed to be basalt-filled rift valleys with very large wrinkle ridges formed over them, possibly in response to flexure from a super-isostatic load of locally thicker basalts (Andrews-Hanna et al., 2014). A similar but smaller linear positive gravity anomaly is located slightly east of and parallel to the northeasternmost and largest wrinkle ridge in western Mare Frigoris. However, the other wrinkle ridges in the parallel set that are farther west across Mare Frigoris do not show significant associated positive gravity anomalies. This may be due to a resolution issue with the available GRAIL gravity data, or the wrinkle ridges are not underlain by thicker basalts. Without a thick basaltic fill to drive subsidence in western Mare Frigoris, faulting could be relatively more sensitive to distal and global stresses.

In addition to the parallel series of degraded wrinkle ridges in western Mare Frigoris are two groups of wrinkle ridges with crisp morphologies (white circles in Fig. 7, also Figs. 9 and 10). The difference in morphological crispness (compare Figs. 2 and 9) suggests a relative age difference, with the crisper ridges being younger than the degraded parallel set. Absolute age estimation by areal crater size frequency distributions is not particularly effective for such small curvilinear features or variable slopes, but crosscutting relationships with small craters can be used to constrain absolute ages of curvilinear landforms. Specifically, craters ~80–100 m in diameter or smaller degrade and infill within ~1 billion years (Trask, 1971; Moore et al., 1980), and can provide maximum age constraints on crosscutting landforms such as wrinkle ridges. Most notably among the ~70 small crosscut craters we identified is a 21 m diameter crater, with bright ejecta, bisected by a small splay off a wrinkle ridge (Fig. 9A). Based on previous crater degradation calibrations, this crater has a modeled age of ~40 million years (Moore et al., 1980). Seismic shaking by the crosscutting fault presumably enhances degradation, so model degradation ages are likely overestimates for small craters crosscut by faults. Since we find that these two groups of crisp wrinkle ridges crosscut small craters < 100 m in diameter, we conclude that these crisp mare wrinkle ridges have been active within the past 1 billion years, and some of these wrinkle ridges have likely been active as recently as within the past ~40 million years.

The distribution and orientations of small graben in Mare Frigoris suggest that they formed as a secondary effect of thrust faulting in wrinkle ridge and lobate scarp formation (Plescia and Golombek, 1986; Watters, 1988; Watters et al., 2012; French et al., 2015). We consider a horizontal 2D strain ellipse such that two zones have line shortening, while the other two would have line lengthening. Thus, dilation occurs

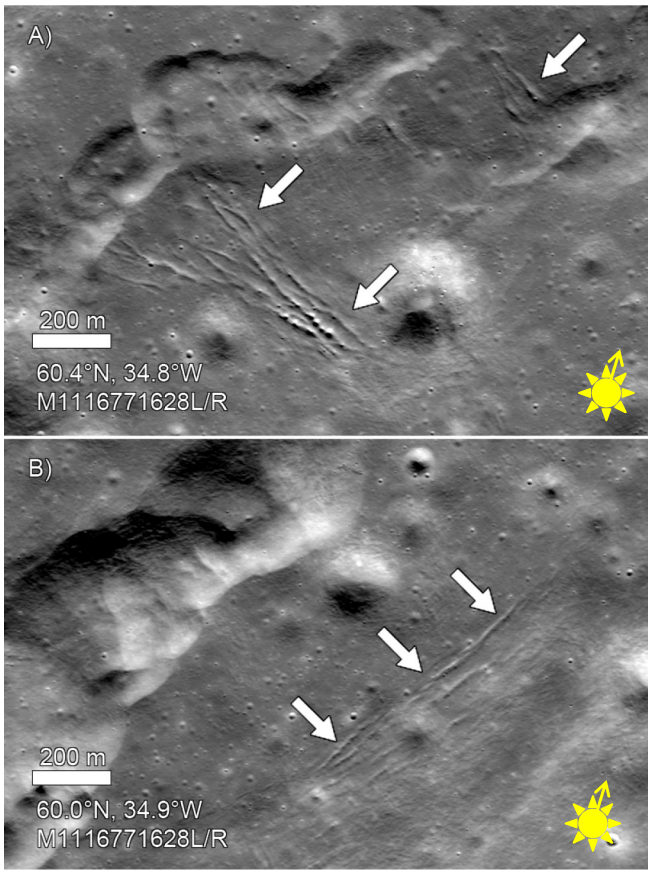


Fig. 12. LROC NAC images showing small graben (arrows) associated with wrinkle ridges. The graben in A) are nearly perpendicular to the associated wrinkle ridge (French et al., 2015), and the graben in B) are nearly parallel to the associated wrinkle ridge.

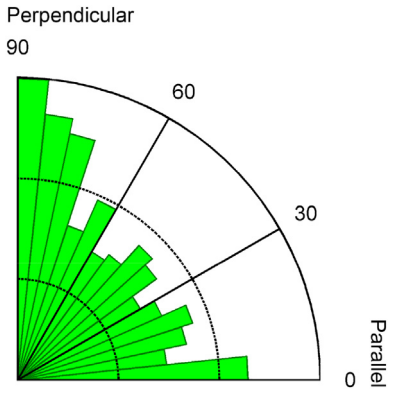


Fig. 13. Azimuthal angle differences between graben and nearest ridge/scarp. Preferred orientations are perpendicular and possibly to a lesser extent parallel.

orthogonal to the shortening axis (the axis corresponding the maximum compressive stress direction) of the strain ellipse enabling the formation of tension gashes, joints, and/or graben. Alternatively, antiformal flexural bending and uplift may also enhance extension of upper-surface material in the same direction as compression on an underlying thrust fault such that graben can preferentially form with their long axes parallel to their host wrinkle ridges. Non-preferred, intermediate orientations are also possible but less preferred due to regolith complexity, pre-existing structures or weaknesses in the substrate, and fault tip effects (Stein, 1999).

Similar to Watters et al. (2012) and French et al. (2015), the small graben observed in Mare Frigoris are typically only a few meters in width and have approximate depths of ~1 m. Based on infilling rates of 2–8 cm/million years for shallow depressions in lunar regolith (Arvidson et al., 1975), they should be filled within ~12.5–50 million years like other examples of small graben globally. Their preservation and incomplete filling implies that not only are the graben very young, but also that wrinkle ridge faults likely causing the associated flexure must have been active within the past few tens of millions of years, and indeed could still be active today. Small graben have also been identified in association with some lobate scarps in the highlands, and some wrinkle ridges in other mare basins (Watters et al., 2012; French et al., 2015) implying that recent wrinkle ridge activity is not restricted to Mare Frigoris. Although a comparable high resolution (few meters/pixel) tectonic mapping campaign has not yet been performed covering all maria and wrinkle ridges globally, we predict that young wrinkle ridge activity is widespread.

A young age for the crisp wrinkle ridges is further supported by the transitions between some wrinkle ridges and young (< 1 billion years old) lobate scarps at mare-highland boundaries. These transitions occur both in Mare Frigoris (e.g., Fig. 4) and at other locations globally including the Lee-Lincoln scarp (Schmitt and Cernan, 1973; Scott, 1973; Lucchitta, 1976a, 1976b; Watters and Johnson, 2010). Thrust faults that underlie both wrinkle ridges and lobate scarps are probably continuous where they cross the mare-highland boundary. Slip on segments of a continuous fault surface likely deforms overlying material on both sides of the mare-highland boundary. Young mare wrinkle ridges at transitions are therefore inferred to deform contemporaneously with highland lobate scarps, consistent with the young ages implied by small crosscut craters and within the established scarp age range of < 1.0 billion years (Binder and Gunga, 1985; Watters et al., 2010). The difference in surface expressions between wrinkle ridges and lobate scarps most likely represents a change in material properties due to layering (Lucchitta, 1976a, 1976b; Watters, 1988, 1991). Based on lobate scarps' and wrinkle ridges' similar ages and examples of continuous transitions between the two morphologic endmembers across geologic terrains, we propose that both lobate scarps and the young subset of wrinkle ridges (white circles in Fig. 7) form from the same compressional stress resulting from the same process.

The young apparent age (< 1 Ga) of crisp wrinkle ridges in western Mare Frigoris does not fit the classical mascon flexure model. In addition, the strong preferred orientations are inconsistent with mascon flexure. The greatest isostatic compensation occurs soon after basalt emplacement, which in Mare Frigoris mostly occurred between ~3.4 and 3.8 billion years ago, with the youngest remnant volcanism ceasing by ~2.6 billion years ago (Hiesinger et al., 2010). Although early flexure induced subsidence is a possible explanation for the initiation of some faults, such ancient flexure is expected to be insufficient to result in significant recent additional displacement. However, a small component of the total stress contributed by subsidence cannot be excluded and could locally influence orientations of some young wrinkle ridges.

Although the primary focus of our study was structures internal to Mare Frigoris, we identified numerous lobate scarps in the highlands adjacent to the mare (example in Fig. 3C, mapped in Fig. 6 as blue lines between 40°E and 50°E). We observe that these lobate scarps have crisp morphologies and crosscut small (< 100 m diameter) craters consistent with a young age (< 1 billion years), similar to observations of other lobate scarps observed in Mare Frigoris and globally as reported in previous studies (Binder and Gunga, 1985; Watters et al., 2010; Banks et al., 2012). No overall spatial pattern is observed for the lobate scarps in the limited highlands area surveyed, with the exception of the large series of lobate scarps just to the east of the mare (Figs. 6, 8). Series of similarly trending lobate scarps are common on the Moon, but the particularly large cumulative length (> 300 km) and sub-parallel paired structure comprising this series east of the mare are noteworthy. The preferential outward-facing lobate scarp faces suggest that the thrust faults dip inwards towards the center of the series. Numerous

small graben occur in the back limbs and in between the scarps indicating localized secondary extension; the spatial correlation further supports a young age for lobate scarps. Such long, paired thrust faults are suggestive of deeper structural control; however, no evidence of such an underlying structure in visible images, topography, or gravity anomaly data was found.

The Apollo lunar seismic network recorded 28 shallow "moonquakes" between 1971 and 1976, distinguished from numerous deep-sourced events and impacts by the shallow quakes' high frequencies. Old boulder falls near some lobate scarps have been proposed to have occurred due to seismicity on lobate scarp faults at Schrodinger basin and in Taurus-Littrow Valley, although the boulder falls have not been seen actively and may also have been due to impact-generated seismicity instead (Arvidson et al., 1975; Kumar et al., 2016). The moment magnitude 2.7 (Oberst, 1987) shallow moonquake recorded on Dec. 6th, 1972, presents an interesting case. Nakamura et al. (1979) located this moonquake epicenter at 51°N, 45°E, after assuming a 100 km depth and suggests that shallow moonquakes may be sourced in the upper lunar mantle (< 200 km), although the event could have been closer to the surface. This places it geographically to within 65 km (~2°) of the 300 km long series of lobate scarps east of Mare Frigoris. The locations of the reported epicenter are not precise to 1°, but should be accurate within a few degrees. A more recent seismic inversion by Lognonné et al. (2003) calculated depths for 7 of the shallow moonquakes, of which five were between 0 and 21 km depth with three between 0 and 2 km depth. The specific moonquake in our study area was not included in Lognonné et al.'s inversion due to its small size and distance outside the Apollo seismic network, but could have been similarly shallow. Watters et al. (2017, manuscript in prep.) found a surface solution to this moonquake using an algorithm for sparse seismic networks. Such shallow calculated depths are also consistent with recent modeling of lobate scarps' maximum fault depths of ~1 km (Williams et al., 2013). The apparent spatial and temporal correlation of this shallow moonquake with these very crisp lobate scarps is consistent with ongoing surface tectonism on the Moon.

Energy released from recorded shallow seismic events and observed strain from lobate scarps can be compared to test if the observed young tectonic landforms could have produced the recorded level of shallow seismicity on the Moon. Strain and seismic energy release are empirically related by $M_0 = 2\mu dA\varepsilon$, where M_0 is the geodetic moment, μ is the shear modulus, d is fault depth, A is surface area, and ε is strain (Savage and Simpson, 1997). Modeling indicates that lobate scarps are shallow with depths d of ~1 km (Williams et al., 2013). We calculate A as the surface area of a sphere with a radius r of 1737.4 km by $A = 4\pi r^2$. The strain ε observed from globally mapped lobate scarps is estimated to be between 0.003% (lower limit) (see Watters et al., 2015) and 0.01% (upper limit) (Watters et al., 2010). The shear modulus can be derived from the shear wave velocity and density by $\mu = V_s^2\rho$, where at 1 km depth, seismic shear wave velocity V_s is 2.8 km/s (Nakamura et al., 1982) and density ρ is 2550 kg/m^3 (Zuber et al., 2013). We divide the total geodetic moment by estimates for the lifetime of the lobate scarp population of 1 billion years (Binder and Gunga, 1985; Watters et al., 2010) and 50 million years (Watters et al., 2015) to obtain estimated annual seismic energy releases of 1.5×10^{14} N-m to 3×10^{15} N-m for 0.01% strain, and 4.5×10^{13} N-m to 9×10^{14} N-m for 0.003% strain. These two estimated ages of strain release bound the observed average seismic energy release of 6.6×10^{14} N m recorded by Apollo (Nakamura et al., 1979; Oberst, 1987). Strain from the mapped global population of young lobate scarps predicts a level of seismicity consistent with the shallow moonquakes recorded during Apollo. Future studies such as a modern seismic network should be directed to detect activity at these young lunar tectonic landforms.

The global population of lobate scarps, predominantly in the highlands, suggests that the Moon's surface is under several MPa of net compressive stress likely resulting from a small amount of global thermal contraction (Binder and Gunga, 1985; Pritchard and Stevenson; Watters et al., 2010; Williams et al., 2013) with a lesser contribution of a few kPa by tidal stresses (Watters et al., 2015) and possibly local stresses from isostatically uncompensated terrain indicated by free-air gravity anomalies (Zuber et al., 2013). The concurrent timing of wrinkle ridges and lobate scarps and the occurrence of ridge–scarp transitions at mare–highland boundaries strongly suggests a shared stress source between associated landforms. We propose that these new young mare wrinkle ridges – akin to highland lobate scarps – also accommodate stress and strain from primarily global thermal contraction with secondary contributions from tidal stresses.

6. Summary

Mare Frigoris is host to a complex assortment of tectonic landforms that imply a complex history of deformation spanning the last ~3.8 billion years. Mare basalts filled most of the eastern part of the mare from ~3.8 to 3.6 billion years ago (Hiesinger et al., 2010), leading to isostatic flexure and subsidence. The center of the eastern mare underwent compression forming the observed polygonal pattern of wrinkle ridges, while the edges of the eastern mare underwent extension forming large linear to arcuate graben. Mare basalts were mostly emplaced in the western mare from ~3.6 to 3.4 billion years ago with some as late as ~2.6 billion years ago (Hiesinger et al., 2010) and were shortly followed by the formation of a parallel set of wrinkle ridges. These ridges do not support mascon induced flexure nor a tectonic control associated with Mare Imbrium. Instead, they suggest a regional, non-isostatic stress field of similar large scale to the previously proposed Procellarum basin, but not necessarily due to impact (Whitaker, 1981) or rifting (Andrews-Hanna et al., 2014). Flexural induced subsidence and resulting tectonic activity decayed and ceased after ~3.4 billion years ago in most places and everywhere in Mare Frigoris after ~2.6 billion years ago, while bombardment of meteoroids progressively degraded these older landforms. Small graben associated with these older landforms may have formed while they were active, but any that might have existed would have been infilled by impact gardening over millions to billions of years.

More recently, in the late Eratosthenian to Copernican (~1 billion years ago), late-stage stresses from global radial contraction formed new faults and perhaps reactivated some old ones. These faults formed lobate scarps in the highlands, including the long cluster just east of Mare Frigoris. New wrinkle ridges formed in the mare and appear in LROC images as a morphologically crisp population contrasting with the older, more degraded ridges. In some cases, new faults crossed the mare-highland boundary forming wrinkle ridge – lobate scarp transitions. Small graben also formed recently as a secondary effect of wrinkle ridge and lobate scarp growth, and at least some have survived to today. Although direct evidence of surface tectonic deformation has not yet been observed in the modern day, the young ages of many tectonic landforms identified globally as well as in Mare Frigoris, along with the shallow moonquakes recorded by Apollo, suggest that tectonic activity is likely still occurring on the lunar surface today.

Acknowledgments

We gratefully acknowledge the LRO, LROC, and GRAIL teams. We especially thank Mark Robinson for targeting and acquiring the LROC NAC images that enabled this study, and Manoochehr Shirzaei for assisting with the comparison of geodetic versus Apollo seismic moments. We also thank the two anonymous reviewers for their constructive feedback on this manuscript. Part of this research was carried out at the Jet Propulsion Laboratory, California Institute of Technology, under a contract with the National Aeronautics and Space Administration. This work was supported by NASA Earth and Space Science Fellowship PLANET14R-0006.

References

Anderson, J.A., Sides, S.C., Soltesz, D.L., Sucharski, T.L., Becker, K.J., 2004. Modernization of the integrated software for imagers and spectrometers. Lunar Planet. Sci. Conf. 35, #2039.

Andrews-Hanna, J.C., Besserer, J., Head, J.W., Howett, C.J.A., Kiefer, W.S., Lucey, P.J., McGovern, P.J., Melosh, H.J., Neumann, G.A., Phillips, R.J., Schenk, P.M., Smith, D.E., Solomon, S.C., Zuber, M.T., 2014. Structure and evolution of the lunar Procellarum region as revealed by GRAIL gravity data. Nature 514, 68–71.

Arvidson, R., Drozd, R.J., Hohenberg, C.M., Morgan, C.J., Poupeau, G., 1975. Horizontal transport of the regolith, modification of features, and erosion rates on the lunar surface. Moon 13, 67–79.

Banks, M.E., Watters, T.R., Robinson, M.S., Tornabene, L.L., Tran, T., Ojha, L., Williams, N.R., 2012. Morphometric analysis of small-scale lobate scarps on the moon using data from the lunar reconnaissance orbiter. J. Geophys. Res. 117. https://doi.org/10.1029/2011JE003907.

Berens, P., 2009. CircStat: a Matlab toolbox for circular statistics. J. Stat. Softw. 31 (10), 2009.

Binder, A.B., Gunga, H.-C., 1985. Young thrust-fault scarps in the highlands: evidence for an initially totally molten moon. Icarus 63, 421–441.

Byrne, P.K., Klimczak, C., McGovern, P.J., Mazarico, E., James, P.B., Neumann, G.A., Zuber, M.T., Solomon, S.C., 2015. Deep-seated thrust faults bound the Mare Crisium lunar mascon. Earth Planet. Sci. Lett. 427, 183–190.

Cadogan, P.H., 1974. Oldest and largest lunar basin? Nature 250, 315–316.

Cadogan, P.H., 1975. The gargantuan basin – some implications. Lunar Planet. Sci. Conf. 6, 123–124.

Freed, A.M., Melosh, H.J., Solomon, S.C., 2001. Tectonics of mascon loading: resolution of the strike-slip faulting paradox. J. Geophys. Res. Planets 106, 20603–20620.

French, R.A., Bina, C.R., Robinson, M.S., Watters, T.R., 2015. Small-scale lunar graben: distribution, dimensions, and formation processes. Icarus 252, 95–106.

Gilbert, G.K., 1893. The Moon's face, a study of the origin of its features. Bull. Philos. Soc. Wash. 12, 241–292.

Golombek, M.P., 1979. Structural analysis of lunar grabens and the shallow crustal structure of the moon. J. Geophys. Res. 84, 4657–4666.

Golombek, M.P., Plescia, J.B., Franklin, B.J., 1991. Faulting and folding in the formation of planetary wrinkle ridges. Proc. Lunar Planet Sci. Conf. 21, 679–693.

Golombek, M.P., Anderson, F.S., Zuber, M.T., 2001. Martian wrinkle ridge topography: evidence for subsurface faults from MOLA. J. Geophys. Res. 106, 23811–23821.

Hiesinger, H., Head, J.W., Wolf, U., Jaumann, R., Neukum, G., 2003. Ages and stratigraphy of mare basalts in Oceanus Procellarum, Mare Nubium, Mare Cognitum, and Mare Insularum. J. Geophys. Res. 108, E75065.

Hiesinger, H., Head, J.W., Wolf, U., Jaumann, R., Neukum, G., 2010. Ages and stratigraphy of the lunar mare basalts in Mare Frigoris and other nearside maria based on crater size-frequency distribution measurements. J. Geophys. Res. 115. https://doi.org/10.1029/2009JE003380.

Howard, K.A., Muehlberger, W.R., 1973. Lunar thrust faults in the Taurus – Littrow region. In: Apollo 17 Prel. Sci. Rep., NASA Spec. Publ. SP-330, pp. 31-22–31-25.

Kirk, R.L., Stevenson, D.J., 1989. The competition between thermal contraction and differentiation in the stress history of the moon. J. Geophys. Res. 12133–12144 B9.

Kumar, S.P., Sruthi, U., Krishna, N., Lakshmi, K.J.P., Menon, R., Aitabh, Krishna, B.G., Kring, D.A., Head, J.W., Goswami, J.N., Kumar, A.S.K., 2016. Recent shallow moonquake and impact-triggered boulder falls on the moon: new insights from the Schrödinger basin. J. Geophys. Res. Planets 121. https://doi.org/10.1002/2015JE004850.

Lemoine, F.G., Goossens, S., Sabaka, T.J., Nicholas, J.B., Mazarico, E., Rowlands, D.D., Loomis, B.D., Chinn, D.S., Neumann, G.A., Smith, D.E., Zuber, M.T., 2014. GRGM900C: a degree 900 lunar gravity model from GRAIL primary and extended mission data. Geophys. Res. Lett. 41 (10), 3382–3389.

Lognonné, P., Gagnepain-Beyneix, J., Chenet, H., 2003. A new seismic model of the moon: implications for structure, thermal evolution, and formation of the moon. Earth Planet. Sci. Lett. 211, 27–44.

Lucchitta, B.K., 1976a. Mare ridges and related highland scarps – result of vertical tectonism? Proc. Lunar Planet. Sci. Conf. 7, 2761–2782.

Lucchitta, B.K., 1976b. Mare ridges and related highland scarps: results of vertical tectonism. Geochim. Cosmochim. Acta 3, 2761–2782 Suppl.

Lucchitta, B.K., Watkins, J.A., 1978. Large grabens and lunar tectonism. Proc. Lunar Planet. Sci. Conf. 9, 666–668.

McGill, G.E., 1971. Attitude of fractures bounding straight and arcuate lunar rilles. Icarus 14, 53–58.

Melosh, H.J., 1978. The tectonics of mascon loading. Proc. Lunar Planet. Sci. Conf. 9, 3513–3525.

Moore, H.J., Boyce, J.M., Hahn, D.A., 1980. Small impact craters in the lunar regolith – their morphologies, relative ages, and rates of formation. Moon Planets 23, 231–252.

Mueller, K., Golombek, M.P., 2004. Compressional structures on Mars. Annu. Rev. Earth Planet. Sci. https://doi.org/10.1146/annurev.earth.1132.101802.120553.

Nakamura, Y., Latham, G.V., Dorman, H.J., Ibrahim, A.-B.K., Koyama, J., Horvath, P., 1979. Shallow moonquakes: depth, distribution and implications as to the present state of the lunar interior. Proc. Lunar Sci. Conf. 10, 2299–2309.

Nakamura, Y., Latham, G.V., Dorman, H.J., 1982. Apollo lunar seismic experiment – final summary. J. Geophys. Res. 87 (Supplement), A117–A123.

Nelson, D.M., Koeber, S.D., Daud, K., Robinson, M.S., Watters, T.R., Banks, M.E., Williams, N.R., 2014. Mapping lunar maria extents and lobate scarps using LROC image products. Lunar Planet. Sci. Conf. 45, 2861.

Neumann, G.A., Zuber, M.T., Wieczorek, M.A., Head, J.W., Baker, D.M.H., Solomon, S.C., Smith, D.E., Lemoine, F.G., Mazarico, E., Sabaka, T.J., Goossens, S.J., Melosh, H.J., Phillips, R.J., Asmar, S.W., Konopliv, A.S., Williams, J.G., Sori, M.M., Soderblom, J.M., Miljkovic, K., Andrews-Hanna, J.C., Nimmo, F., Kiefer, W.S., 2015. Lunar impact basins revealed by gravity recovery and interior laboratory measurements. Sci. Adv. 1, e1500852. https://doi.org/10.1126/sciadv.1500852.

Oberst, J., 1987. Unusually high stress drops associated with shallow moonquakes. J. Geophys. Res. 92 (B2), 1397–1405.

Plescia, J.B., Golombek, M.P., 1986. Origin of planetary wrinkle ridges based on the study of terrestrial analogs. Geol. Soc. Am. Bull. 97, 1289–1299.

Pritchard, M.E., Stevenson, D.J., 2000. Thermal aspects of a lunar origin by giant impact. In: Canup, R., Righter, K. (Eds.), Origin of the Earth and Moon. University of Arizona Press, Tucson, AZ, pp. 179–196.

Robinson, M.S., Brylow, S.M., Tschimmel, M., Humm, D., Lawrence, S.J., Thomas, P.C., Denevi, B.W., Bowman-Cisneros, E., Zerr, J., Ravine, M.A., Caplinger, M.A., Ghaemi, F.T., Schaffner, J.A., Malin, M.C., Mahanti, P., Bartels, A., Anderson, J., Tran, T.N., Eliason, E.M., McEwen, A.S., Turtle, E., Jolliff, B.L., Hiesinger, H., 2010. Lunar Reconnaissance Orbiter Camera (LROC) instrument overview. Space Sci. Rev. 150, 81–124.

Savage, J.C., Simpson, R.W., 1997. Surface strain accumulation and the seismic moment tensor. Bull. Seismol. Soc. Am. 87 (5), 1345–1353.

Schmitt, H.H., Cernan, E.A., 1973. Geological investigation of the Apollo 17 landing site. In: Apollo 17 Preliminary Sci. Report. NASA Spec. Publ. SP-330, pp. 5-1–5-21.

Scholten, F., Oberst, J., Matz, K.-D., Roatsch, T., Wahlish, M., Speyerer, E.J., Robinson, M.S., 2012. GLD100: the near-global lunar 100 m raster DTM from LROC WAC stereo image data. J. Geophys. Res. Planets 117. https://doi.org/10.1029/2011JE003926.

Schultz, R.A., 2000. Localizaton of bedding-plane slip and backthrust faults above blind thrust faults: keys to wrinkle ridge structure. J. Geophys. Res. 105 (12), 035–12 052.

Scott, D.H., 1973. Small structures of the Taurus-Littrow region. In: Apollo 17 Preliminary Sci. Report. NASA Spec. Publ. SP-330, pp. 31-25–31-29.

Smith, D.E., Zuber, M.T., Jackson, G.B., Cavanaugh, J.F., Neumann, G.A., Riris, H., Sun, X., Zellar, R.S., Coltharp, C., Connelly, J., Katz, R.B., Kleyner, I., Liiva, P., Matuszeski, A., Mazarico, E.M., McGarr, J.F., Novo-Gradac, A.-M., Ott, M.N., Peters, C., Ramos-Izquierdo, L.A., Ramsey, L., Rowlands, D.D., Schmidt, S., Scott, V.S., Shaw, G.B., Smith, J.C., Swinski, J.-P., Torrence, M.H., Unger, G., Yu, A.W., Zagwodzki, T.W., 2010. Lunar Orbiter Laser Altimeter on the Lunar Reconnaissance Orbiter Mission. Space Sci. Rev. 150, 209–241.

Solomon, S.C., Head, J.W., 1979. Vertical movement in mare basins: relation to mare emplacement, basin tectonics and lunar thermal history. J. Geophys. Res. 84, 1667–1682.

Solomon, S.C., Head, J.W., 1980. Lunar mascon basins: lava filling, tectonics, and evolution of the lithosphere. Rev. Geophys. Space Phys. 18, 107–141.

Stein, R.S., 1999. The role of stress transfer in earthquake occurrence. Nature 402, 605–609.

Trask, N.J., 1971. Geologic Comparison of Mare Materials in the Lunar Equatorial Belt, Including Apollo 11 and Apollo 12 Landing Sites. 750-D. pp. D138–D144 (US Geol. Survey Prof. Paper).

Watters, T.R., 1988. Wrinkle ridge assemblages on the terrestrial planets. J. Geophys. Res. 93, 10236–10254.

Watters, T.R., 1991. Origin of periodically spaced wrinkle ridges on the Tharsis Plateau of Mars. J. Geophys. Res. Planets 96 (E1), 15599–15616.

Watters, T.R., 1992. A system of tectonic features common to Earth, Mars, and Venus. Geology 20, 609–612.

Watters, T.R., 2004. Elastic dislocation modeling of wrinkle ridges on Mars. Icarus 171, 284–294.

Watters, T.R., Johnson, C.L., 2010. Lunar tectonics. In: Watters, T.R., Schultz, R.A. (Eds.), Planetary Tectonics. Cambridge University Press, Cambridge, UK, pp. 121–182.

Watters, T.R., Robinson, M.S., Beyer, R.A., Banks, M.E., Bell, J.F., Pritchard, M.E., Hiesinger, H., van der Bogert, C.H., Thomas, P.C., Turtle, E.P., Williams, N.R., 2010. Evidence of recent thrust faulting on the Moon revealed by the Lunar Reconnaissance Orbiter Camera. Science 329, 936–940.

Watters, T.R., Robinson, M.S., Banks, M.E., Tran, T., Denevi, B.W., 2012. Recent extensional tectonics on the Moon revealed by the Lunar Reconnaissance Orbiter Camera. Nat. Geosci. 5, 181–185.

Watters, T.R., Robinson, M.S., Collins, G.C., Banks, M.E., Daud, K., Williams, N.R., 2015. Global thrust faulting on the moon and the influence of tidal stresses. Geology 43 (10), 851–854.

Watters, T.R., Weber, R.C., Collins, G.C., Johnson, C.L., 2017. Shallow lunar seismic activity and the current stress state of the moon. In: 48th Lunar and Planetary Science Conference, manuscript in prep. (Abstract #2569).

Whitaker, E.A., 1981. The lunar Procellarum basin. In: Schultz, P.H., Berrill, R.B. (Eds.), Multi-ring Basins. vol. 12A. pp. 105–111 Proc. Lunar Planet. Sci. Conf.

Whitford-Stark, J.L., 1981. Modification of multi-ring basins – the Imbrium model. In: Schultz, P.H., Berrill, R.B. (Eds.), Multi-ring Basins. vol. 12A. pp. 113–124 Proc. Lunar Planet. Sci. Conf.

Whitford-Stark, J.L., 1990. The volcanotectonic evolution of Mare Frigoris. Proc. Lunar Planet. Sci. Conf. 20, 175–185.

Wieczorek, M.A., Neumann, G.A., Nimmo, F., Kiefer, W.S., Taylor, G.J., Melosh, H.J., Phillips, R.J., Solomon, S.C., Andrews-Hanna, J.C., Asmar, S.W., Konopliv, A.S., Lemoine, F.G., Smith, D.E., Watkins, M.M., Williams, J.G., Zuber, M.T., 2013. The crust of the moon as seen by GRAIL. Science 339, 671–675.

Wilhelms, D.E., 1987. The Geologic History of the Moon. U.S. Government Printing Office, Washington, DC.

Williams, N.R., Watters, T.R., Pritchard, M.E., Banks, M.E., Bell, J.F., 2013. Fault dislocation modeled structure of lobate scarps from Lunar Reconnaissance Orbiter Camera digital terrain models. J. Geophys. Res. 118, 224–233.

Zuber, M.T., Smith, D.E., Watkins, M.M., Asmar, S.W., Konopliv, A.S., Lemoine, F.G., Melosh, H.J., Neumann, G.A., Phillips, R.J., Solomon, S.C., Wieczorek, M.A., Williams, J.G., Goossens, S.J., Kruizinga, G., Mazarico, E., Park, R.S., Yuan, D.-N., 2013. Gravity field of the moon from the Gravity Recovery and Interior Laboratory (GRAIL) mission. Science 339, 668–671.